Unfaulting of dislocation loops in the GaInNAs alloy: An estimation of the stacking fault energy

M. Herrera, D. González,[a] J. G. Lozano, and R. García
Departamento de Ciencia de los Materiales e Ingeniería Metalúrgica y Química Inorgánica, Universidad de Cádiz, Apartado 40, 11510 Puerto Real, Cádiz, Spain

M. Hopkinson, H. Y. Liu, M. Gutierrez, and P. Navaretti
Department of Electronic and Electrical Engineering, University of Sheffield, Mappin Street, Sheffield S1 3JD, United Kingdom

(Received 16 November 2004; accepted 3 June 2005; published online 29 July 2005)

A study by transmission electron microscopy of the influence of the In and N contents in the ranges of 20%–35% and 1.1%–3%, respectively, on the microstructure of $Ga_{1-x}In_xN_yAs_{1-y}$ quantum wells is presented. Frank dislocation loops characterized as extrinsic have been found in the samples with $x \geqslant 0.25$. In these structures, threading dislocations appear as a consequence of the unfaulting of the loops for $y \geqslant 0.014$. An analysis of the density and size of the dislocation loops has provided an estimation of the critical radius for the unfaulting process. A model for this critical radius of the unfaulting process of extrinsic Frank loops is proposed. From this model and experimental values of critical radius, an estimation of the stacking fault energy of the GaInNAs alloy has been made. We have found a reduction in the stacking fault energy of the GaInNAs alloys when increasing the N content from 1.4% to 2.3% in good agreement with the theoretical estimation of the stacking fault energies of zinc-blende GaN and InN. © *2005 American Institute of Physics*.
[DOI: 10.1063/1.1988976]

I. INTRODUCTION

In the recent years, quaternary alloys of GaInNAs have attracted considerable attention as promising materials for edge-emitting[1] as well as vertical-cavity surface-emitting[2,3] lasers and for efficient solar cells.[4] The differences in size and electronegativity between N and the other column-V elements result in an alloy with unique properties such as a strong negative bowing parameter, which causes a huge decrease of the band gap by the addition of relatively small amounts of N ($<5\%$) to GaInAs.[5] Access to wavelengths in the 1.0–1.55 μm range makes this material system attractive for lasers. Moreover, this alloy has been proposed[5] to overcome the low characteristic temperature (T_0) due to a poor electron confinement from the small conduction-band offset of the conventional system GaInAsP/InP.

The role of the introduction of N in the GaInAs alloy is twofold: on the one hand, it reduces the band gap, mainly by acting on the conduction band and, secondly, the small size of the N atoms reduces the lattice parameter of the GaInNAs alloy and consequently the lattice mismatch with GaAs substrates. Therefore, fewer structural defects are expected compared to the GaInAs alloys with the same In fraction. In order to obtain the highest optical quality for long-wavelength emission an optimization of the In and N compositions is essential. In general, this is pursued through an improvement in the efficiency of luminescence. However, few studies have been published regarding the structural defects that appear in high In- and N-content GaInNAs heterostructures. Moreover, although intensive efforts are being applied to the characterization of this alloy, basic properties, such as its stacking fault energy per unit area γ, remain unknown. This work is focused on the mechanisms of defect generation that take place in high In- and N-content GaInNAs quantum wells. Our results have allowed us to make an estimation of the γ of these GaInNAs alloys finding that γ follows a negative trend with the increase of N content.

II. EXPERIMENT

The samples have been grown by molecular-beam epitaxy (MBE) on (001) GaAs substrates in a VG V80H MBE system equipped with an Oxford Applied Research HD25 radio-frequency plasma source for N. The N flux was controlled by monitoring the intensity of the atomic N plasma emission with a photodiode. The nitrogen content in the epilayers was calibrated from the x-ray-diffraction analysis of bulk samples and GaNAs quantum wells grown using similar plasma emission intensities. The growth temperature was 460 °C throughout the quantum well region. Five 8-nm GaInNAs quantum wells (QWs), with In and N contents in the 20%–35% and 1.3%–3% ranges, respectively, were sandwiched between $GaN_{0.007}As$ barriers of 52-nm width. The QW structure was capped with 200 nm of GaAs and 200 nm of Al_4Ga_6As, at growth temperatures of 580 and 620 °C, respectively. After the AlGaAs growth, the sample was left at 620 °C for 1 h under As overpressure. The purpose of this anneal step is to improve the photoluminescence intensity which is generally low in as-grown samples. Using this step the photoluminescence (PL) intensity is observed to increase by factors of 5–20, depending on the composition. However, no major change in the PL linewidth or the x-ray-diffraction

[a]Electronic mail: david.gonzalez@uca.es

TABLE I. In and N contents of the studied GaInNAs quantum wells.

Sample	%In	%N
A20-1.3	20	1.3
A25-1.6	25	1.6
A35-1.1	35	1.1
A35-1.4	35	1.4
A35-2.3	35	2.3
A35-3	35	3.0

data from the samples is observed, suggesting no significant structural change. The particular In and N compositions in each sample are shown in Table I.

Specimens were prepared by mechanical thinning followed by Ar^+-ion milling for cross-sectional (CS) and planar view (PV) transmission electron microscopy (TEM) analyses. TEM studies were performed with JEOL EX1200 and JEOL 2011 microscopes.

III. RESULTS

Planar quantum wells without structural defects have been observed in the TEM study of sample A20-1.3, with the lowest In and N contents (20% and 1.3%, respectively). On increasing the In composition to 25% (sample A25-1.6), the surface of the wells becomes undulated, with a wavelength of undulation of about 20 nm. This feature is accompanied by the formation of dislocation loops, which present a regular distribution in all the QWs of the structure. The existence of dislocation loops in GaInNAs has been reported by others,[6,7] but no detailed structural characterization has yet been reported. Our contrast diffraction study revealed that they are Frank dislocation loops (FDLs) being characterized by the inside-outside contrast criterion[8,9] as extrinsic. For higher In contents (35%), besides the three-dimensional (3D) morphology and the extrinsic dislocation loops [shown in PVTEM in Fig. 1(a) for sample A35-1.4), threading dislocations (TDs) have been observed, as are shown in Fig. 1(b) for sample A35-2.3 in CSTEM. The Burgers vector of the threading dislocations has been characterized by the invisibility criterion. The results of this study have shown that approximately one-third of the dislocations have Burgers vector $\frac{1}{2}a\langle 101]$, one-third $\frac{1}{2}a\langle 011]$, and the remaining ones $\frac{1}{2}a\langle 110]$. The details of the characterization of these dislocations have been published in a previous paper.[10] It is worth mentioning that misfit dislocations have not been observed in these samples, neither in the cross-section study nor in the planar view one. An analysis of the TD density and the density and size of the dislocation loops in relation to the N composition in the samples with 35% In content has been developed. With regards to the TDs, these are absent in lower N-content sample A35-1.1, appearing on increasing the N composition to 1.4% and 2.3%. However, it should be mentioned that the density of TDs in these samples is somewhat lower for higher N contents, given that we have measured a density of TDs of $3.5\pm0.5\times10^9$ cm^{-2} for A35-1.4 and of $1.5\pm0.5\times10^9$ cm^{-2} for A35-2.3. Structure A35-3 shows poor crystal quality, with a very high density of TDs reflecting the difficulty of achieving high N content while preserving good crystal quality.

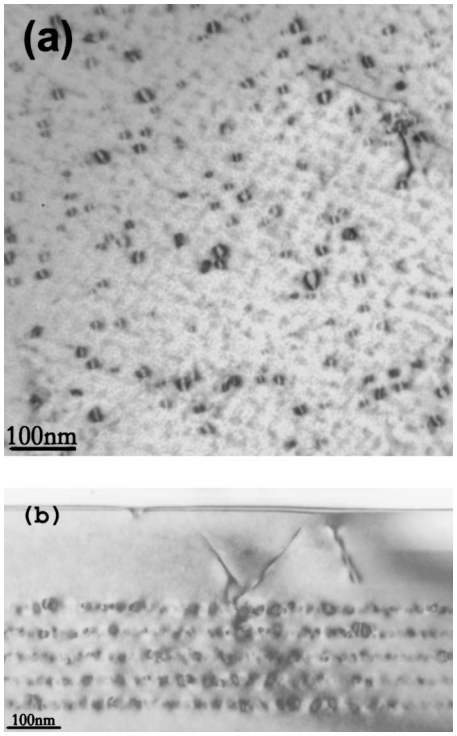

FIG. 1. (a) PV micrograph with 220BF reflection of sample A35-1.4, showing the appearance of dislocation loops. (b) CS image of structure A35-2.3 taken with 220BF reflection, where threading dislocations are exhibited. We can also observe the regular distribution of the FDL in all QWs of the structure.

Measurements of density and size of the dislocation loops in samples A35-1.1, A35-1.4, and A35-2.3 have been performed in the planar view TEM study. Regarding the experimental procedure, it should be noted that the FDLs are regularly distributed in the five quantum wells [see Fig. 1(b)], but in the observation in PV it is not easy to recognize how many wells are being studied in a particular area of the sample preparation. In order to be able to compare the density of Frank dislocation loops (ρ_{FDL}) obtained in the different structures, we have first measured the ρ_{FDL} in each well in CS, and these data have been used to select an area of the specimen foil in PV where all the wells are observed at the same time. This analysis showed that the density of loops is similar in each of the five quantum wells. Following this procedure, the size distribution of the dislocation loops has been measured. Figure 2 shows histograms of the radii of the loops in samples A35-1.4 and A35-2.3. As it can be observed, the distribution of radii is displaced to higher values when increasing the N content, with the average sizes of the loops approximately 13 and 16 nm for 1.4% and 2.3% N, respectively. Moreover, the ρ_{FDL} is also higher for higher N compositions, having global surface densities (comprising the five quantum wells) of $1.3\pm0.3\times10^{10}$ and $2.0\pm0.3\times10^{10}$ cm^{-2}, respectively. In sample A35-1.1, the density of FDLs is much lower than in the higher N-content samples (1.5×10^8 cm^{-2}) and all the FDLs have radii in the range of 7–12 nm.

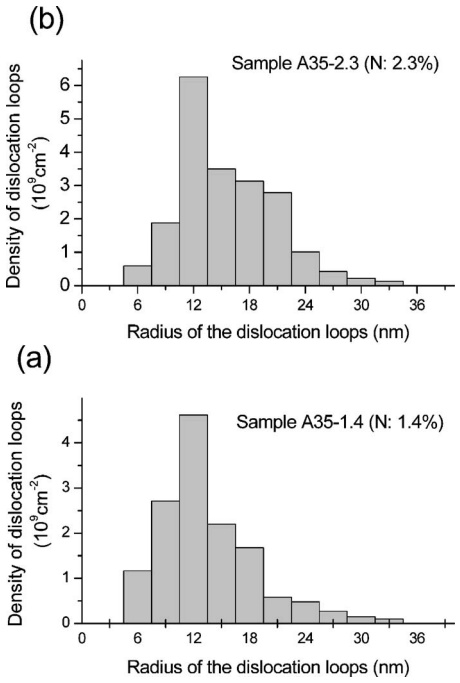

FIG. 2. Histograms of the surface density of dislocation loops vs the radius of the loops for samples A35-1.4 (a) and A35-2.3 (b).

Attention should be paid to the distribution of radii in the histograms in Figs. 2(a) and 2(b). As it can be seen, there is one interval with a density of loops, which is rather high, centered at 12 nm for both samples. On increasing the radii of the FDLs, the amount of defects in each interval is progressively diminished. However, in this progression it can be observed that it is one step larger than the other ones. For sample A35-1.4, this step is located at 21.5 ± 1.5 nm, and the difference in ρ_{FDL} between those intervals of the histogram is more than two times higher than that observed in the values of radius of 13.5, 22.5, 25.5, 28.5 nm, etc. In sample A35-2.3, the abnormally high step is placed at 24 ± 1.5 nm, and the reduction in ρ_{FDL} is three times higher than that found in the remaining intervals. It seems that there could be a mechanism of disappearance of loops with radii higher than the values observed. This mechanism will be discussed later.

IV. DISCUSSION

A. The unfaulting process

Beginning with the influence of the In composition in the microstructure of the GaInNAs quantum wells, we have observed that the appearance of Frank dislocation loops is closely related to the undulation of the surface of the wells when increasing the In content from 20% to 25%. In general, these types of defects originate by the accumulation of point defects (vacancies for intrinsic type or interstitials for extrinsic type) due to a diffusion-controlled process. For the case of island growth, Cullis *et al.*[11] have reported that Frank loops may form by vacancy aggregation in the compressive stress field of a valley due to the associated partial relaxation of the local stress. In this sense, the level of point defects is probably the key point to explain the different behavior between GaInNAs and GaInAs QWs. Several authors have demonstrated that there is a significant percentage of interstitial N (Refs. 12–14) and In (Ref. 15) in as-grown GaInNAs samples and that the annealing process removes these, either to substitutional sites or to the surface. They also propose that strain at the interfaces plays an important role in interstitial behavior. In our samples, the local stress concentrations associated with interface undulations could trigger the collapse of interstitial defects in the fault planes that act as the origin of the FDLs.

On the other hand, threading dislocations have been observed in samples with 35% of In. The characterization of these TDs has shown that approximately one-third has Burgers vector of $\frac{1}{2}a\langle 101]$, one-third $\frac{1}{2}a\langle 011]$, and one-third $\frac{1}{2}a\langle 110]$. This result implies that despite two-thirds of the dislocations having the typical 60° Burger vector out of the growth plane, one-third of them has 60° Burgers vector lying in the growth plane. In order to understand the mechanisms of the formation of these dislocations, we have calculated the curve of critical layer thickness for plastic relaxation according to the classical model of Matthews-Blakeslee.[16] This calculation showed that the thickness of the GaInNAs wells is lower than the critical value; therefore, the formation of dislocations by the Matthews-Blakeslee mechanism[16] is not energetically favorable in these samples.

Our TEM study shows that no conventional misfit dislocation (MD) array is observed such as that common in III-V systems such as GaInAs/GaAs. In these systems, dislocations glide due to the mismatch stress forming long straight segments at the interface that relieve the strain in the overlying region. In the case of strained multiple layers (SMLs), this MD network is generally located at the first interface and its density depends on the SML thickness and the lattice mismatch. The absence of misfit relief mechanisms in our analyses implies that the TDs are not associated with MD generation.

An alternative process for the appearance of the observed threading dislocations is the unfaulting of the existing dislocation loops transforming these to perfect loops that would later glide to the surface of the structure. This hypothesis is in agreement with the fact that most of the dislocations found in the PVTEM and CSTEM studies are grouped in pairs, departing from the same point (see Fig. 1). In Fig. 3 we observe a perfect loop that extends up towards the surface [Fig. 3(a)] and the probable final half-loop configuration [Fig. 3(b)]. The unfaulting process through which a Frank loop transforms into a perfect loop by the coalescence reaction with Shockley partial dislocations has been widely reported.[17,18] In the particular case of extrinsic FDLs, two Shockley partials are needed for the unfaulting mechanism (see Ref. 19 and references therein). In fcc structures, the habit plane of Frank dislocation loops is {111} type because of the lower stacking fault energy (γ). In these {111} planes, there are three possible Shockley partial dislocations that could take part in the coalescence reaction with the loop. The reactions between an interstitial FDL and each pair of these partial dislocations can be expressed as

$$\frac{a}{6}[\bar{1}2\bar{1}] + \frac{a}{6}[\bar{1}\bar{1}2] + \frac{a}{3}[111] \rightarrow \frac{a}{2}[011],$$

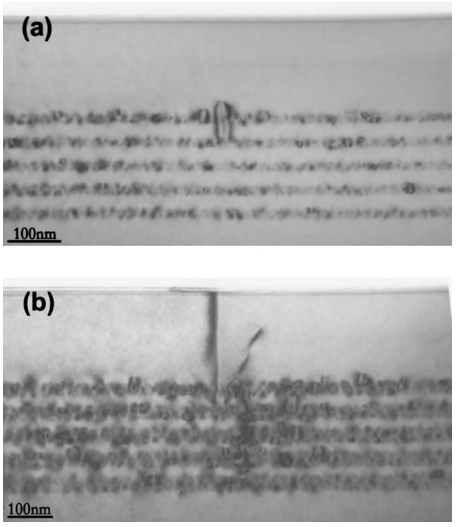

FIG. 3. CS micrographs in the 220BF reflection of sample A35-1.4. (a) shows a perfect dislocation loop that drives up to the surface and (b) shows a loop that exhibits the probable half-loop configuration formed by the unfaulting process.

$$\frac{a}{6}[\bar{1}\bar{1}2]+\frac{a}{6}[2\bar{1}\bar{1}]+\frac{a}{3}[111]\rightarrow\frac{a}{2}[101], \tag{1}$$

$$\frac{a}{6}[2\bar{1}\bar{1}]+\frac{a}{6}[\bar{1}2\bar{1}]+\frac{a}{3}[111]\rightarrow\frac{a}{2}[110].$$

As it can be observed, the result of the reaction of a Frank extrinsic dislocation loop with two Shockley partial dislocations is the formation of a perfect dislocation, with one of these three Burgers vectors. The probability of occurrence of these three reactions in the materials should be the same, therefore the unfaulting of the FDLs gives place to perfect dislocations, one-third with each of the Burgers vector result of the reactions above, which includes one-third of dislocations with Burgers vector 60° lying in the growth plane. This agrees with the experimental results obtained in the study of the GaInNAs quantum wells with 35% In and high N contents, therefore, it can be concluded that the mechanism of the formation of the observed threading dislocations is the unfaulting of the dislocation loops to form perfect dislocations that glide to the surface of the structure.[10] This process is determined by γ and by the radius of the FDLs. In the following, we discuss the energetic involved in the unfaulting process of a Frank dislocation loop, to permit us to calculate the stacking fault energy of the GaInNAs system.

B. Model of unfaulting of interstitial Frank loops

The classical model to describe the energies involved in the unfaulting process of Frank dislocation loops starts from the comparison of the formation energies of the FDLs and the perfect loops.[20,21] The formation energy of a FDL comprises the stacking fault energy of the loop E_{SF} and the elastic energy of line dislocations $E_{l,\mathrm{Frank}}$. On the other hand, the formation energy of a perfect dislocation loop with circular shape and Burgers vector **b** can be expressed as the sum of the energies of two dislocation loops with Burgers vectors in the loop plane ($\mathbf{b}_{in}$) and out of it ($\mathbf{b}_{out}$), respectively, providing $\mathbf{b}=\mathbf{b}_{in}+\mathbf{b}_{out}$. In the following, we assume for simplicity elastically isotropic bodies with homogeneous composition, which is determined by a single lattice parameter a and, as a first approximation, which follows Vegard's rule. Thus, the unfaulting process occurs when

$$E_{SF}+E_{l,\mathrm{Frank}}=E_{l,\mathrm{perfect}}, \tag{2}$$

being

$$E_{SF}=\pi r^2\gamma, \tag{3}$$

$$E_{l,\mathrm{Frank}}=2\pi r\frac{\mu b_{\mathrm{Frank}}^2}{4\pi(1-\nu)}\left[\ln\left(\frac{8\alpha r}{b_{\mathrm{Frank}}}\right)-1\right], \tag{4}$$

$$E_{l,\mathrm{perfect}}=2\pi r\frac{\mu b_{\mathrm{out}}^2}{4\pi(1-\nu)}\left[\ln\left(\frac{8\alpha r}{b_{\mathrm{out}}}\right)-1\right]+2\pi r\frac{2-\nu}{2(1-\nu)}\frac{\mu b_{\mathrm{in}}^2}{4\pi}\left[\ln\left(\frac{8\alpha r}{b_{\mathrm{in}}}\right)-2\right], \tag{5}$$

where r is the radius of the dislocation loop, μ is the shear modulus, ν is the Poisson ratio, a is the dislocation core factor, and b_{Frank} is the Burgers vector modulus of the Frank dislocation loop. We consider the values of the lattice parameter, shear modulus, and Poisson modulus obtained from the extrapolation of those corresponding to the binaries, taken into account the values of the zinc-blende phase of the GaN and InN.[22] In our case, $b_{\mathrm{Frank}}=b_{\mathrm{out}}=a/\sqrt{3}$ and $b_{\mathrm{in}}=a/\sqrt{6}$. Therefore, we can obtain the relationship between the critical radius for the unfaulting process r_{crit} and γ as

$$\gamma=\frac{\mu a^2}{24\pi r_{\mathrm{crit}}}\frac{2+\nu}{(1-\nu)}\left[\ln\left(\sqrt{6}\frac{\alpha r_{\mathrm{crit}}}{a}\right)\right]. \tag{6}$$

From Eq. (6) we can obtain a value of γ for sample A35-2.3 of 83.5 $\mathrm{mJ/m^2}$. This value is notably high compared to the γ of $Ga_{0.65}In_{0.35}As$ calculated by the extrapolation from the values of the binaries,[23] which is about 38.5 $\mathrm{mJ/m^2}$. The addition of small amounts of nitrogen can modify the stacking fault energy of the GaInAs system, but we would expect a reduction instead of an increase. The reason is the stability of the wurtzite structure of the III-N compounds compared to the zinc-blende structure. The increase of N content favors the trend of a wurtzite stacking inside the zinc-blende structure and this fact should signify a fall in the γ. In addition, the classic model does not distinguish between the intrinsic and the extrinsic case, the critical radius is the same in both cases. Nevertheless, the conditions for the unfaulting process are very different. For a Frank vacancy loop (intrinsic), the unfaulting process occurs by the formation of a partial Shockley dislocation that glides in an energetically favorable direction. However, the unfaulting process of a Frank interstitial loop (extrinsic) implies a displacement in an energetically unfavorable direction and it is necessary to a synchronic shear of two Shockley partials that glide at the bottom and top atomic planes of the loop, respectively.[24] This reasoning is in agreement with the fact that no large Frank vacancy loops have been observed in the widely studied irra-

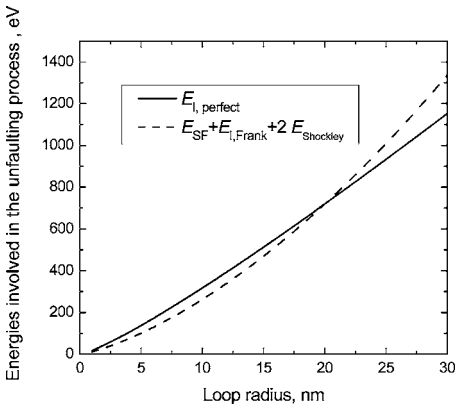

FIG. 4. Plot of the energies involved in the unfaulting process of an interstitial Frank dislocation loop in sample A35-2.3 vs the radius of the loop. The Frank dislocation loops are stable for radius below 20 nm and the unfaulting to perfect loops becomes spontaneous for radius above.

diated austenitic stainless steels and only the interstitial ones have been found.[25]

Taking the above into account, we think that the energetic treatment of the unfaulting process is more accurate if we also consider the formation energy of the two Shockley partial dislocations that glide in different planes. Thus, we can write the energetic balance of the global process as

$$E_{\text{SF}} + E_{l,\text{Frank}} + 2E_{\text{Shockley}} = E_{l,\text{perfect}}, \tag{7}$$

being

$$E_{\text{Shockley}} = 2\pi r \frac{\mu b_{\text{Shockley}}^2}{4\pi}\left[\cos(\beta)^2 - \frac{\sin(\beta)^2}{1-\nu}\right]\ln\left(\frac{\alpha r}{b_{\text{Shockley}}}\right), \tag{8}$$

where β is the angle between the Burgers vector and the dislocation line for the Shockley segments, being in our case $\beta=\pi/6$ and $b_{\text{Shockley}}=a/\sqrt{6}$. Note that we consider the Shockley partial dislocations as straight segments and not as loops, although the total dislocation line formed is the length of the loop circle.

To check the model, we have calculated the critical radius for the unfaulting process in the GaInNAs alloy from Eq. (7) above and we have compared the results with our experimental findings. However, there are no experimental values for the stacking fault energies for the cubic structure in the case of GaN or InN. Only Wright,[26] using density-functional-theory calculations, has estimated the energies of zinc-blende stacking faults for the group-III nitrides. The values for GaN ($\gamma_{\text{GaN}}=-50.2$ mJ/m^2) and InN ($\gamma_{\text{InN}}=-62.7$ mJ/m^2) are both negative values which are justified by the difficulty of growing pure cubic III-N materials.

Figure 4 shows a plot the formation energy of the two terms in the energetic balance of the unfaulting process from Eq. (7) for the case of sample A35-2.3. As it can be observed, Frank dislocation loops with radii relatively small (lower than ~20 nm) can be stable in the material. However, on increasing their size, the accumulated γ is raised as well, and the unfaulting process becomes favorable. As a result, the relative stability of perfect and Frank dislocation loops is directly linked to the size of the defect. In relation to this, the experimental results of the distribution of the size of the loops for samples A35-1.4 and A35-2.3 (Figs. 2(a) and 2(b), respectively) have shown a sudden reduction in the density of loops when reaching the values of the radius of 21.5 ± 1.5 and 24 ± 1.5 nm, respectively. Considering the reasoning above, this finding suggests that the decrease in FDLs observed in our experimental study could be due to loops having reached their critical radius for the process of unfaulting. A considerable number of FDLs, with radii higher than the critical values (21.5 nm for A35-1.4 and 24 nm for A35-2.3), unfault to give rise to the threading dislocations observed in our study. Table II shows the critical radii for samples A35-1.4 and A35-2.3 found experimentally and calculated using the proposed model. As it can be clearly seen, there is an excellent agreement for the two samples analyzed. In sample A35-1.1, however, TDs were not found. This could be explained by the small size of the loops in this sample, which are unlikely to reach the critical radius for the unfaulting process for these In and N compositions.

TABLE II. Experimental critical radius of unfaulting of FDLs and theoretical γ_{theor} using the $\gamma_{\text{III-N}}$ data proposed by Wright (Ref. 22) for samples A35-1.4 and A35-2.3. For the same samples, critical radius (using γ_{theor} and γ_{expt} (using experimental critical radius) calculated with the proposed unfaulting model.

Sample	r_{crit} (Expt.)(nm)	r_{crit} (Model) (nm)	γ_{expt}(mJ/m^2)	γ_{theor}(mJ/m^2)
A35-1.4	21.5 ± 1.5	19.26	34 ± 2	37.1
A35-2.3	24 ± 1.5	20.20	31 ± 2	36.3

As explained above, the critical radius of the dislocation loops for the process of unfaulting is directly related to the γ of the material. We are going to use the experimental values of critical radius obtained in our study to estimate the γ of the GaInNAs alloy. From Eq. (7) we can obtain an expression for the γ implicated in the unfaulting process of an extrinsic loop as

$$\gamma = \frac{\mu a^2}{4800\pi\, r_{\text{crit}}(1-v)}\left[400v\,\ln\left(\frac{\alpha\, r_{\text{crit}}}{a}\right) + 32 + 343v\right]. \tag{9}$$

From this equation, a critical radius of a loop of 21.5 nm (sample A35-1.4, $Ga_{0.65}In_{0.35}N_{0.014}As_{0.986}$ alloy) corresponds to a γ of the material of 34 ± 2 mJ/m^2. Similarly, for the $Ga_{0.65}In_{0.35}N_{0.023}As_{0.977}$ alloy (sample A35-2.3) a value of the γ of 31 ± 2 mJ/m^2 is calculated. As it can be observed, the consequence of the introduction of N in the GaIn(N)As alloy is a reduction in the γ of the material in agreement with the theoretical predictions using the $\gamma_{\text{III-N}}$ proposed by Wright[26] although our experimental results show high γ decay with the nitrogen content than the theoreticals. This could mean a greater contribution of the stacking fault energy of the III-N binaries than that expected in the global γ, that is to say, the real $\gamma_{\text{III-N}}$ values are higher than that estimated by Wright. In addition, the possibility that a high concentration of the N atoms occurs in local areas of the structure, reducing significantly the stacking fault energy in these regions, should also be considered. In previous papers,[27,28]

TABLE III. Summary of the main results obtained in the study of the dislocation loops and threading dislocations in the samples with 35% In: global surface density of dislocation loops (ρ_{FDL}), average radius of the loops (r_{av}), critical radius (r_{crit}), stacking fault energy (γ), and density of threading dislocations (ρ_{TD}).

Sample	%N	f	r_{av} (nm)	ρ_{FDL} (cm^{-2})	r_{crit} (nm)	γ (mJ/m^2)	ρ_{TD} (cm^{-2})
A35-1.1	1.1	0.0228	11.0	1.5×10^{8}			
A35-1.4	1.4	0.0222	13.4	1.3×10^{10}	21.5±1	34±2	3×10^{9}
A35-2.3	2.3	0.0204	15.5	2.0×10^{10}	24±1.5	31±2	2×10^{9}
A35-3	3.0	0.0191	⋯	⋯	⋯	⋯	$>10^{10}$

we have shown the existence of composition modulation in the ⟨110⟩ directions in the growth plane of GaInNAs structures. This fact supposes a source of error in the stacking fault energy determinations. Up to now, several authors have already reported the experimental data of lateral composition modulation amplitude for GaInNAs QWs.[29–31] Albrecht *et al.*[30] reported fluctuations in the concentration of indium of ±0.05 for as-grown samples, but only ±0.01 for the annealed samples. We have estimated that this can provide an increase of about 3% of the absolute error in the stacking fault estimation.

The significance of the decrease of γ found experimentally is that it provides a serious handicap for N-rich GaInNAs growth. The lower the fault energy, the higher are the stacking fault and twin densities in the sample. These features of the microstructure may be considered as precursors to the wurtzite formation.[32] If we could consider valid Vegard's rule for any N content, a sample with 40% of nitrogen would have zero γ and would change from zinc-blende phase to wurtzite phase.

Table III shows a summary of the main results obtained in the present study. As it can be clearly seen, on raising the N content in the alloy both the density of FDLs and their average radii are increased and this behavior leads to TD formation through an unfaulting process. Therefore, from each dislocation loop that unfaults and glides to the surface of the structure, two threading dislocations are formed. It should be highlighted that the density of threading dislocations found in A35-2.3 is slightly lower than that found in A35-1.4. In sample A35-1.4, approximately half of the FDLs with radii higher than the critical one has suffered the process of unfaulting whereas in A35-2.3 only one-third of them has been converted to perfect dislocations. The fact that not all the loops with radii higher than the critical value suffer unfaulting could be due to kinetic limitations. As has been discussed above, the FDL unfaults when it reacts with two Shockley partial dislocations nucleated inside the loop. In the formation and movement of these partial dislocations, local stresses in the structure play an essential role. According to this, the reasons for the higher proportion of loops that unfault in the sample with lower N content, A35-1.4, could be related to the higher lattice mismatch (f) in this structure. An increase in f when reducing the N composition could favor the formation and movement of the Shockley partials in the material, enhancing the probability of unfaulting in agreement with the experimental results obtained for A35-1.4 and A35-2.3. At the other extreme, the N-rich sample showed a high TD density due to the increase on the size and density of FDLs. The extrapolated value of FDL average size will be very close to the critical radius of unfaulting, compensating the small reduction of lattice mismatch.

The presence of a high density of interstitial defects in GaInNAs causes the formation of Frank dislocation loops that subsequently unfault, generating a high density of TD. The expectation of defect-free N-rich GaInNAs structures due to the reduction of lattice mismatch with increasing N content needs to be revised. The defect formation in N-rich GaInNAs is not controlled by the plastic relaxation of the lattice mismatch, but by FDLs generation and a subsequent unfaulting process, which occurs primarily due a decrease in γ.

V. CONCLUSIONS

The unfaulting of extrinsic Frank dislocation loops into perfect loops in GaInNAs alloy has been studied both theoretically and experimentally. By transmission electron microscopy, we have observed Frank loops in $Ga_{1-x}In_xN_yAs$ quantum wells with $x \geqslant 0.25$, and also threading dislocations for $y \geqslant 0.014$, which are generated from the unfaulting of the loops. The analysis of the distribution of size of the loops in samples with 35% In showed a sudden reduction in the density of the loops at radii of 21.5 nm for 1.4%N and 24 nm for 2.3%N. We associate these values with a critical radius for the process of unfaulting. With these experimental values of the critical radius and the theoretical approach proposed by the authors, an estimation of the stacking fault energy for the GaInNAs alloy has been made. For $Ga_{0.65}In_{0.35}N_{0.014}As$, the stacking fault energy has been calculated as 34 mJ/m^2, and for $Ga_{0.65}In_{0.35}N_{0.023}As$, as 31 mJ/m^2. These values are in good agreement with the theoretical estimation found in the bibliography. Therefore, the introduction of N in the GaInNAs alloy reduces the stacking fault energy of the alloy. The defect generation of high N-content GaInNAs samples is governed by the FDL formation and unfaulting processes instead of by plastic relaxation due to lattice mismatch.

ACKNOWLEDGMENTS

Financial supports from CICYT Project No. MAT2001-3362 (Spain), the Spanish Ministry of Education, and EPSRC (UK) are gratefully acknowledged.

[1] S. Illek, A. Ultsch, B. Borchert, A. Y. Egorov, and H. Riechert, Electron. Lett. **36**, 725 (2000).
[2] C. W. Coldren, M. C. Larson, S. G. Spruytte, and J. S. Harris, Electron. Lett. **36**, 951 (2000).
[3] G. Steinle, H. Riechert, and A. Y. Egorov, Electron. Lett. **31**, 93 (2001).

[4]S. R. Kurtz, A. A. Allerman, E. D. Jones, J. M. Gee, and J. J. Banas, Appl. Phys. Lett. **74**, 729 (1999).
[5]M. Kondow, K. Uomi, A. Niwa, T. Kitatani, S. Watahiki, and Y. Yazawa, Jpn. J. Appl. Phys., Part 1 **35**, 1273 (1996).
[6]B. V. Volovik *et al.*, Semicond. Sci. Technol. **16**, 186 (2001).
[7]K. Nakashima and K. Tateno, J. Appl. Phys. **95**, 3443 (2004).
[8]P. Hirsch, A. Howie, R. B. Nicholson, D. W. Pashley, and M. J. Whelan, *Electron Microscopy of Thin Films* (Butterworks, Malabar, FL., 1977).
[9]J. W. Eddington, *Practical Electron Microscopy in Materials Science* (N. V. Philips, Eindhoven, 1975).
[10]M. Herrera, D. González, R. García, M. Hopkinson, P. Navaretti, M. Gutiérrez, and H. Y. Liu, Thin Solid Films (in press).
[11]A. G. Cullis, A. J. Pidduck, and M. T. Emeny, J. Cryst. Growth **158**, 15 (1996).
[12]S. G. Spruytte, C. W. Coldren, J. S. Harris, W. Wampler, P. Krispin, and K. Ploog, J. Appl. Phys. **89**, 4401 (2001).
[13]C. S. Peng, W. Li, T. Jouhti, E. M. Pavelescu, and M. Pessa, J. Cryst. Growth **251**, 378 (2003).
[14]T. Ahlgren, E. Vainonen-Ahlgren, J. Likonen, W. Li, and M. Pessa, Appl. Phys. Lett. **80**, 2314 (2002).
[15]S. L. White *et al.*, Solid-State Electron. **47**, 425 (2003).
[16]J. W. Matthews and A. E. Blakeslee, J. Cryst. Growth **27**, 118 (1974).
[17]J. J. Homes, R. E. Robbins, J. L. Brimhall, and B. Mastel, Acta Metall. **16**, 955 (1968).
[18]F. A. Garner and D. S. Gelles, J. Nucl. Mater. **159**, 286 (1988).
[19]S. G. Song, J. I. Cole, and S. M. Bruemmer, Acta Mater. **45**, 501 (1997).
[20]D. Hull and D. J. Bacon, *Introduction to Dislocations* (Pergamon, New York, 1984).
[21]F. Cristiano, J. Grisolia, B. Colombeau, M. Omri, B. de Mauduit, A. Claverie, L. F. Giles, and N. E. B. Cowern, J. Appl. Phys. **87**, 8420 (2000).
[22]A. F. Wright, J. Appl. Phys. **82**, 2833 (1997).
[23]S. Takeuchi and K. Suzuki, Phys. Status Solidi A **171**, 99 (1999).
[24]E. H. Lee, M. H. Yoo, T. S. Byun, J. D. Hunn, K. Farrell, and L. K. Mansur, Acta Mater. **49**, 3277 (2001).
[25]H. Takahashi, Y. Hidaka, and S. Ohnuki, Micron **27**, 239 (1996).
[26]A. F. Wright, J. Appl. Phys. **82**, 5229 (1997).
[27]M. Herrera, D. González, M. Hopkinson, M. Gutiérrez, P. Navaretti, H. Y. Liu, and R. García, J. Appl. Phys. **97**, 073705 (2005).
[28]M. Herrera, D. González, M. Hopkinson, M. Gutiérrez, P. Navaretti, H. Y. Liu, and R. García, Semicond. Sci. Technol. **19**, 813 (2004).
[29]V. Grillo, M. Albrecht, T. Remmele, H. P. Strunk, A. Yu. Egorov, and H. Riechert, J. Appl. Phys. **90**, 3792 (2001).
[30]M. Albrecht *et al.*, Appl. Phys. Lett. **81**, 2719 (2002).
[31]G. Patriarche, L. Largeau, J. C. Harmand, and D. Gollub, Appl. Phys. Lett. **84**, 203 (2004).
[32]C. Montero-Ocampo, R. Juarez, and A. Salinas Rodríguez, Metall. Mater. Trans. A **33A**, 2229 (2002).